

Chapter 6

Reactive Intermediates Revealed in Secondary Organic Aerosol Formation from Isoprene*

*This chapter is reproduced by permission from “Reactive Intermediates Revealed in Secondary Organic Aerosol Formation from Isoprene” by Jason D. Surratt, Arthur W. H. Chan, Nathan C. Eddingsaas, ManNin Chan, Christine L. Loza, Alan J. Kwan, Scott P. Hersey, Richard C. Flagan, Paul O. Wennberg and John H. Seinfeld, *Proceedings of the National Academy of Sciences of the United States of America*, doi:10.1073/pnas.0911114107, 2009. Copyright 2009 by the National Academy of Sciences.

6.1 Abstract

Isoprene is a significant source of atmospheric organic aerosol; however, the oxidation pathways that lead to secondary organic aerosol (SOA) have remained elusive. Here, we identify the role of two key reactive intermediates, epoxydiols of isoprene (IEPOX = β -IEPOX + δ -IEPOX) and methacryloylperoxynitrate (MPAN), that are formed during isoprene oxidation under low- and high-NO_x conditions, respectively. Isoprene low-NO_x SOA is enhanced in the presence of acidified sulfate seed aerosol (mass yield 28.6%) over that in the presence of neutral aerosol (mass yield 1.3%). Increased uptake of IEPOX by acid-catalyzed particle-phase reactions is shown to explain this enhancement. Under high-NO_x conditions, isoprene SOA formation occurs through oxidation of its second-generation product, MPAN. The similarity of the composition of SOA formed from the photooxidation of MPAN to that formed from isoprene and methacrolein (MACR) demonstrates the role of MPAN in the formation of isoprene high-NO_x SOA. Reactions of IEPOX and MPAN in the presence of anthropogenic pollutants (i.e., acidic aerosol produced from the oxidation of SO₂ and NO₂, respectively) could be a substantial source of “missing urban SOA” not included in current atmospheric models.

6.2 Introduction

Isoprene (2-methyl-1,3-butadiene, C_5H_8) is the most abundant non-methane hydrocarbon emitted into the Earth's atmosphere, with emissions estimated to be 440–660 TgC yr⁻¹ (1). The atmospheric hydroxyl (OH) radical-initiated oxidation of isoprene, so-called photooxidation, plays a key role in establishing the balance of hydrogen oxide ($HO_x = OH + HO_2$) radicals in vegetated areas (2, 3) and influences urban ozone formation in populated areas blanketed with biogenic emissions (4). Formation of low-volatility compounds during isoprene oxidation has been estimated to be the single largest source of atmospheric organic aerosol (i.e., SOA) (5–8).

The photooxidation of unsaturated volatile organic compounds (VOCs) proceeds through formation of a hydroxy peroxy (RO_2) radical, the fate of which depends on the concentration of nitrogen oxides ($NO_x = NO + NO_2$). Higher SOA yields from isoprene are observed under low- NO_x (or NO_x -free) conditions; in this regime, RO_2 radicals react primarily with HO_2 , a pathway that tends to produce lower-volatility oxidation products than that involving the reaction of RO_2 with NO (9–11). Under high- NO_x conditions, RO_2 radicals react with NO to produce alkoxy (RO) radicals, or as a minor pathway, organic nitrates ($RONO_2$). For small VOCs ($\leq C_{10}$), like isoprene, these RO radicals generally fragment into smaller more volatile products, resulting in small amounts of SOA (9–11). Despite the fact that SOA from isoprene has been extensively studied (8), the chemical pathways to its formation under both low- and high- NO_x conditions have remained unclear. In this study we examine the mechanism of isoprene SOA formation in these two limiting regimes.

6.3 Results and Discussion

6.3.1 Isoprene SOA Formation under Low-NO_x Conditions: Role of Aerosol Acidity

Formation of SOA from the photooxidation of isoprene under low-NO_x conditions is enhanced in the presence of acidified sulfate seed aerosol over that in the presence of neutral aerosol (12); this is not observed under high-NO_x conditions since the aerosol phase is likely acidic enough due to the formation and presence of nitric acid (HNO₃) (13) and/or organic acids (12). The effect of increasing aerosol acidity on both gas- and aerosol-phase composition provides a critical clue to the chemical mechanism of SOA formation from isoprene under low-NO_x conditions. Enhancement of isoprene SOA mass with increasing aerosol acidity observed in laboratory chamber studies (12, 14, 15), including increased mass concentrations of the 2-methyltetrols (14, 15), organosulfates of isoprene (i.e., hydroxy sulfate esters) (15), and high-MW SOA constituents (15), has been explained by acid-catalyzed particle-phase reactions. Although a linear correlation between the SOA mass formed and measured aerosol acidity (i.e., nmol H⁺ m⁻³) has been found under dry conditions (~30% RH) (15), the actual acid-catalyzed particle-phase reactions responsible for these observed enhancements in isoprene SOA formation remain unclear, especially since previously proposed reactions, like that of organosulfate formation by alcohol sulfate esterification (16–18), appear to be kinetically unfavorable at atmospheric conditions (19).

Shown in Figure 6.1*A–F* are the chemical ionization mass spectrometry (CIMS) (see Materials and Methods) time traces for selected ions corresponding to the important gas-phase products formed from the photooxidation of 49 and 40 ppb of isoprene in the presence of neutral and highly acidified sulfate seed aerosol, respectively. The SOA

mass yields from isoprene were 1.3% and 28.6% for the neutral and highly acidified sulfate seed aerosol experiments, respectively. Under the conditions of these experiments, the RO₂ radicals formed react primarily with HO₂. In addition to the formation of hydroxycarbonyls, methyl-butenediols, hydroxyhydroperoxides (ISOPOOH), MACR, and methyl vinyl ketone (MVK), all of which are first-generation gas-phase oxidation products (Figure 6.1A–D), we also observe the formation of second-generation IEPOX, as indicated in Figure 6.1F (i.e., 9 ppb and 0.6 ppb of IEPOX was measured in the neutral and acidic cases, respectively). Although the 2-methyltetrols (Figure 6.1E) can be produced from RO₂ radical-cross reactions, their formation through this route is of minor significance (~0.2 ppb) in these experiments owing to the dominant RO₂ + HO₂ pathway. The hydroxycarbonyls (~0.8 ppb) and methyl-butenediols (~0.8 ppb) are first-generation products also formed from RO₂ radical-cross reactions; however, part of the CIMS signal associated with the methyl-butenediols (Figure 6.1B) arises from later-generation oxidation products with the elemental composition C₄H₆O₃, likely a C₄-hydroxydicarbonyl and/or C₄-acid. Hydroxynitrates of isoprene were also observed (< 0.1 ppb). Their formation results from background NO in the chamber. Thus a fraction of the MACR and MVK produced results from RO₂ + NO reactions (~3% of RO₂ radicals reacted with NO).

IEPOX (i.e., δ -IEPOX) was proposed to form from the photooxidation of isoprene under low-NO_x conditions in order to tentatively explain the formation of chemically characterized SOA constituents (12, 20). Gas-phase IEPOX (β -IEPOX and δ -IEPOX) was recently shown to form in substantial yields (upwards of 75%) from the further oxidation of ISOPOOH (~12 ppb measured in both the neutral and acidic cases in Figure

6.1C) by OH under low-NO_x conditions (3). The substantial reduction of gas-phase IEPOX in the presence of highly acidified sulfate seed aerosol (Figure 6.1F) confirms the role of IEPOX in the enhancement of isoprene SOA mass under lower-NO_x conditions at increased aerosol acidity.

Isoprene low-NO_x SOA was analyzed off-line by gas chromatography/electron ionization-quadrupole mass spectrometry (GC/EI-MS) with prior trimethylsilylation and ultra performance liquid chromatography/electrospray ionization-time-of-flight mass spectrometry operated in the negative ion mode (UPLC/(–)ESI-TOFMS) (see Methods and Materials). Particle-phase IEPOX is characterized here for the first time. The GC/EI-MS mass spectra of the trimethylsilyl (TMS)-derivatives of IEPOX associated with the two chromatographic peaks in Figure 6.1G are shown in Figure 6.6. Extracted ion chromatograms (EICs) of selected ions corresponding to particle-phase IEPOX, as well as the previously characterized C₅-alkene triols (20), 2-methyltetrols (5), hemiacetal dimers (12), organosulfate derivatives of the 2-methyltetrols (16, 17), and organosulfate derivatives of the hemiacetal dimers (18) are shown in Figure 6.1G–L, respectively. Mass spectra in the present study for the previously characterized low-NO_x SOA constituents shown in Figure 6.1H–L correspond to those collected in prior work (5, 12, 16, 20), and are shown in Figure 6.6 and Figure 6.7. The abundances of all low-NO_x SOA constituents shown in Figure 6.1G–L are enhanced significantly in the presence of acidified sulfate seed aerosol. Using a suitable surrogate standard (i.e., *meso*-erythritol to quantify the 2-methyltetrols), we estimate that the mass concentrations of these compounds increased from 0.1 μg m^{–3} for the neutral case to 5.1 μg m^{–3} for the highly acidic case, corresponding to ~ 10 to 20%, respectively, of the total SOA mass formed.

6.3.2 Identification of IEPOX as the Intermediate Responsible for Acid-Enhanced Isoprene SOA

We hypothesize that particle-phase reactions of IEPOX play a significant role in the formation of the other major low-NO_x SOA constituents shown in Figure 6.1*H–L*, as well as in the enhancement of total SOA mass. To test this hypothesis, we synthesized 2,3-epoxy-1,4-butanediol (BEPOX) (see Materials and Methods), which is the butadiene derivative of IEPOX, and conducted reactive uptake experiments in the presence of both neutral and highly acidified sulfate seed aerosol. BEPOX is used in these experiments instead of IEPOX, as precursors for IEPOX are not commercially available. In these dark and dry (<10% RH) experiments, no OH precursor (e.g., H₂O₂) or NO_x was present; thus, only reactive uptake of BEPOX onto seed aerosol occurred. Two variations of these reactive uptake experiments were carried out: (1) BEPOX was added first, followed by the injection of seed aerosol; or (2) seed aerosol was added first, followed by the injection of BEPOX. CIMS time traces corresponding to version (1) of the BEPOX reactive uptake experiments are shown in Figure 6.2*A*. The only parameter varied was the acidity of the sulfate seed aerosol. BEPOX is rapidly removed from the gas phase within the first hour after the acidified sulfate seed aerosol is injected into the well-mixed chamber. Upon the injection of neutral sulfate seed aerosol, BEPOX disappears from wall loss only and not reactive uptake. Once the injection of gas-phase BEPOX ended (indicated at time zero in Figure 6.2*A*), it decayed at similar rates before either the neutral or highly acidified sulfate seed aerosol was injected. The clear conclusion is that BEPOX loss to the highly acidic seed aerosol results from acid-catalyzed particle-phase reactions.

SOA formed in the acidified BEPOX reactive uptake experiments shown in Figure 6.2*A* was collected for off-line chemical analyses by GC/EI-MS and UPLC/(–

)ESI-TOFMS (Figure 6.8). In addition to sharing similar retention times (RTs), the mass spectrum of the TMS-derivative of the particle-phase BEPOX (Figure 6.8) corresponds exactly to that of the synthesized BEPOX standard (see Figure 6.9). The major chromatographic peak observed in the EIC of m/z 248 (Figure 6.8) is attributable only to particle-phase BEPOX, whereas the two later-eluting minor peaks represent background contributions. The other major SOA constituents characterized from the reactive uptake of BEPOX are also exact analogues of isoprene SOA formed under low- NO_x conditions (i.e., differing by a mass of 14 Da, which corresponds to a CH_2 group); these include: C_4 -alkene triols, tetrols (i.e., threitol and erythritol), dimers, organosulfate derivatives of the tetrols, and organosulfate derivatives of the dimers (Figure 6.8). Equivalent to the low- NO_x isoprene SOA (Figure 6.1G–L), these BEPOX SOA constituents were significantly enhanced under increased seed aerosol acidity, consistent with the rapid removal of gas-phase BEPOX onto the highly acidified sulfate seed aerosol. The tetrols (i.e., threitol and erythritol) were quantified by GC/EI-MS and their summed mass was found to increase from 43 ng m^{-3} to $1.3 \text{ } \mu\text{g m}^{-3}$ from neutral to highly acidic conditions.

In version (2) of the BEPOX reactive uptake experiments, within the first hour after the addition of BEPOX, the sulfate aerosol mass concentration decayed more rapidly (by $\sim 58\%$ of its initial loading) in the highly acidic case than that which could be explained by wall loss alone, indicating depletion of the inorganic sulfate through chemical reaction with BEPOX (Figure 6.10). A similar observation made in isoprene SOA formation (16) is consistent with the reactive uptake of IEPOX forming organosulfates of isoprene. The SOA mass generated after the injection of gas-phase BEPOX increased from 0.9 to $15.8 \text{ } \mu\text{g m}^{-3}$ from neutral to acidified sulfate seed aerosol.

Importantly, organosulfates of BEPOX (i.e. organosulfate derivatives of the tetrols and dimers, as well as higher order organosulfates shown in Figure 6.11) were also characterized in these experiments (Figure 6.8). We conclude from these observations that conversion of inorganic sulfate into organosulfates occurs by the acid-catalyzed ring opening of the epoxydiols followed by the subsequent nucleophilic addition of inorganic sulfate.

Reactive uptake onto acidified sulfate seed aerosol also occurs when BEPOX and IEPOX are formed from butadiene and isoprene photooxidation, respectively. 100 ppb of butadiene and 50 ppb of isoprene were initially irradiated in the absence of seed aerosol (Figure 6.2*B* and Figure 6.2*C*, respectively). Once sufficient gas-phase levels of both BEPOX and IEPOX formed, seed aerosol was injected. For the butadiene experiment (Figure 6.2*B*), only highly acidified sulfate seed aerosol was injected. Because hydroxyhydroperoxides and BEPOX, gas-phase oxidation products of butadiene, are isomers both detected by the CIMS technique at m/z 189, characteristic daughter ions produced from m/z 189 were used to differentiate between these two compounds. The daughter ions at m/z 63 and 169 are uniquely characteristic of the hydroxyhydroperoxide and BEPOX, respectively (3). Upon the injection of acidified sulfate seed aerosol, BEPOX was the only oxidation product rapidly removed from the gas-phase mixture (decayed by ~75% within the first hour after seed aerosol was injected). The SOA constituents from butadiene shown in Figure 6.2*B* are precisely those shown in Figure 6.8. In the case of isoprene photooxidation (Figure 6.2*C*), as observed for the BEPOX reactive uptake and butadiene photooxidation (Figure 6.2*A* and 6.2*B*, respectively), gas-phase IEPOX disappeared significantly only in the presence of acidified sulfate seed

aerosol (Figure 6.2C). Moreover, the constituents characterized in the SOA formed from the latter experiment are precisely those shown in Figure 6.1G–L.

6.3.3 Mechanism of Isoprene SOA Formation under Low-NO_x Conditions

An updated chemical mechanism for SOA formation from isoprene under low-NO_x conditions is shown in Figure 6.3. The gas-phase formation of IEPOX has been fully characterized by Paulot et al. (3). Here we have established that the reactive uptake of IEPOX occurs by the acid-catalyzed ring opening of this epoxydiol, followed by the subsequent addition of the following nucleophiles: (1) H₂O; (2) inorganic sulfate; (3) a 2-methyltetrol already formed in the aerosol; and (4) a hydroxy sulfate ester already present in the aerosol. Unreacted particle-phase IEPOX observed in the isoprene SOA is likely a result of equilibrium gas-to-particle partitioning. Although the formation of 2-methyltetrols has been detected from the further oxidation of methyl-butenediols under conditions in which RO₂ + RO₂ reactions dominate (at large isoprene mixing ratios, i.e., 8–12 ppmC) (21), the atmospheric formation of the 2-methyltetrols will occur primarily via the further reaction of IEPOX as shown in Figure 6.3, since the HO₂ concentration exceeds that of all RO₂ radicals (22) and because rate coefficients of RO₂ + RO₂ reactions are usually smaller than those for RO₂ + HO₂ reactions (23). The organosulfates of isoprene are shown conclusively to form from the reactive uptake of IEPOX, rather than by the previously proposed alcohol sulfate esterification mechanism (18). This conclusion is consistent with recent work by Iinuma et al. (24), who showed organosulfates of α- and β-pinene form through the reactive uptake of α- and β-pinene oxides, only in the presence of acidified sulfate seed aerosol. Additionally, recent work

has shown that organosulfate formation is kinetically favorable only for epoxides and not for alcohols at atmospherically relevant conditions (19).

Although the C₅-alkene triols were observed in these experiments, their exact formation mechanism remains unclear. We cannot rule out the possibility that these compounds are produced from the trimethylsilylation step prior to GC/EI-MS analysis, as a TMS-derivative of the synthesized BEPOX standard was found to have a contribution from C₄-alkene triols. Preliminary results suggest that these compounds are more abundant than the tetrols under high RH conditions. Enhanced C₅-alkene triol concentrations have been observed when transitioning from the dry to wet seasons in the Amazon (20). Finally, the dimers previously observed in both laboratory-generated isoprene SOA and organic aerosol collected from the Amazon are likely not a result of hemiacetal formation (12); rather these dimers are shown to form from polymerization of IEPOX by acid-catalyzed ring opening of IEPOX.

6.3.4 Isoprene SOA Formation under High-NO_x Conditions: Role of MPAN

The majority of the high-NO_x SOA yield from isoprene has previously been traced to the oxidation of a major (25% yield (25)) first-generation oxidation product of isoprene, MACR (9, 12). Providing further evidence of the role of MACR, the chemical composition of the SOA produced in the oxidation of MACR is similar to that found in studies of the oxidation of isoprene, especially 2-methylglyceric acid (2-MG), a C₄-dihydroxycarboxylic acid, which undergoes esterification to produce low-volatility oligoesters (12, 26). Both 2-MG and its corresponding diester have been observed in ambient aerosol samples (7).

The preservation of the four-carbon backbone in the SOA produced following the oxidation of MACR provides significant constraints on the gas-phase mechanism that yields the SOA precursor. Oxidation of MACR by OH proceeds both via addition to the double bond (~55%) and abstraction of the aldehydic hydrogen (45%) (27, 28). Preservation of the carbon backbone generally precludes formation of RO radicals as they rapidly decompose to form hydroxyacetone (via OH addition) and methylvinyl radicals (via aldehydic abstraction) (28). This suggests that, following abstraction of the aldehydic hydrogen by OH, formation of MPAN is likely key to SOA production. MPAN is formed from MACR with a maximum yield of ~45% (27, 29). Following addition of OH to the double bond, the only known gas-phase mechanism that prevents C-C fragmentation in the presence of NO_x is the channel leading to the formation of a hydroxynitrate (7, 27, 30). Thus, to oxidize both the double bond and the aldehydic hydrogen, one route to C₄ preservation leads to the formation of the hydroxynitrate of MPAN. Alternatively, the addition of OH to MPAN might lead to the formation of bridged oxygen compounds if the alkyl radical (or subsequent RO₂ or RO radicals) rearrange unimolecularly and decompose by breaking off the weak peroxyxynitrate moiety forming peroxy or epoxy carbonyls.

To test the hypothesis that the formation of MPAN is key for SOA formation, MACR was oxidized by OH (formed via HONO photolysis) in the presence of a very high concentration of NO (>500 ppb). Under these conditions, the peroxyacyl radical formed following H-abstraction (and addition of O₂) reacts primarily with NO to form formaldehyde, CO and CO₂ rather than with NO₂ to form MPAN (27, 29). Although formation of hydroxynitrate was observed from the addition channel (~10–15% of

hydroxyacetone), little SOA was produced (mass yield <2%). SOA yields (2.9% from 257 ppb MACR) were higher when 290 ppb of NO was added, and highest (5.1% from 285 ppb MACR) when 350 ppb of additional NO₂ (instead of NO) was injected. As shown in Figure 6.12, the relative aerosol-phase concentrations of oligoesters are also enhanced under higher [NO₂]/[NO] ratios, consistent with the trends observed in SOA yields from MACR photooxidation. The RTs and molecular formulas match those of the oligoester products formed in isoprene high-NO_x SOA. NO levels remained above 120 ppb during the course of all the experiments, and thus RO₂ + HO₂ and RO₂ + RO₂ reactions are not competitive. HONO levels, as measured by CIMS, were within 15% among these experiments. The observed increase in SOA at higher NO₂ levels is also unlikely to be a result of condensation of nitric acid from OH + NO₂ reactions, as addition of gas-phase nitric acid did not lead to additional aerosol growth. The observed effect of [NO₂]/[NO] ratio on oligoester formation and overall aerosol yields in MACR photooxidation suggests the importance of peroxyxynitrate formation via an RO₂ + NO₂ pathway. In the chamber, the lifetime of MPAN against thermal decomposition is about 100 min (31), and can be effectively much longer under higher [NO₂]/[NO] ratios, as the peroxyacyl radicals formed following thermal decomposition react preferentially with NO₂ reforming MPAN.

6.3.5 Identification of MPAN as Key Intermediate in Formation of SOA from Isoprene and MACR

To verify the hypothesis that the route to high-NO_x SOA formation from isoprene goes through MPAN, experiments were carried out with synthesized MPAN (see Materials and Methods). When MPAN was injected into the chamber in the presence solely of ammonium sulfate seed, SOA was not observed. Significant aerosol growth

was observed only upon photooxidation of MPAN (with photolysis of HONO used as the OH source). Moreover, as shown in Figure 6.4, the composition of SOA formed from MPAN oxidation was similar to that from high-NO_x photooxidation of MACR and isoprene. In particular, 2-MG and its corresponding oligoesters are identified in all three aerosol samples using both GC/EI-MS and UPLC/(-)ESI-TOFMS. Detailed chemical characterization of 2-MG and its corresponding oligoesters (12, 26) and similar analysis of the current samples confirm the presence of these products in aerosol formed from MPAN oxidation (Figure 6.4 and Table 6.1). Other aerosol components found in isoprene SOA, such as compounds with a C₅-hydroxynitrate backbone, are not found in MACR or MPAN SOA, but their contribution to total aerosol mass is likely small, and their formation mechanisms have been tentatively established (18). We confirmed that 2-MG and its corresponding oligoesters are formed as a result of MPAN oxidation and not an impurity (i.e., methacrylic acid) (see Supporting Information).

Additional experiments provide insight into the mechanism by which 2-MG is formed from the OH reaction of MPAN. Oxidation of 2-methyl-3-buten-2-ol (MBO), structurally similar to isoprene, but lacking the second double bond, leads to no aerosol formation. This suggests that formation of 2-MG requires OH reaction with the double bond of MPAN. OH addition to the MPAN double bond, followed by addition of O₂, leads to formation of an RO₂ radical; under the chamber conditions, reaction with NO is most likely, leading to formation of either an RO radical or a C₄-hydroxynitrate-PAN. Owing to the 2-position of the alkoxy group, this C₄-alkoxy radical is unlikely to undergo traditional H-atom transfer isomerization, and therefore decomposes rapidly to break the C₄-backbone. One possibility is that 2-MG is formed through the C₄-hydroxynitrate-PAN

channel (see Figure 6.5). Dommen et al. (32) observed lower-volatility isoprene SOA (which is consistent with the formation of oligomers) to form under dry rather than humid conditions, which is consistent with a mechanism that involves decomposition of the C₄-hydroxynitrate-PAN into 2-MG and allows for subsequent esterification of 2-MG into the observed oligoesters. We do not, however, have conclusive chemical evidence to support the hypothesis that the C₄-hydroxynitrate-PAN is the main precursor to the isoprene high-NO_x SOA. Indeed, there is some evidence that this is not the route. A signal, comparable in magnitude to the hydroxynitrate of MACR (at *m/z* 234) and highly correlated to the time trace of SOA formation, is observed at *m/z* 311 – a mass consistent with the cluster of CF₃O⁻ with the C₄-hydroxynitrate-PAN. Assuming the same CIMS response factor as glycolaldehyde, the signal at *m/z* 311 is consistent with all of the C₄-hydroxynitrate-PAN being accounted for in the gas phase (assuming the yield of the C₄-hydroxynitrate from MPAN is comparable to the yield of the hydroxynitrate from MACR), and as a result, this compound could not be the SOA precursor. Thus, it is possible that some unknown C₄-preserving chemical reaction is occurring when MPAN is oxidized by OH (e.g., similar to the formation of IEPOX under low-NO_x conditions, the OH-MPAN radical adduct intramolecularly rearranges into a highly-strained epoxide before O₂ adds).

The OH reaction rate constants of saturated peroxyacyl nitrates (PANs) are sufficiently small ($< 1 \times 10^{-13} \text{ cm}^3 \text{ molec}^{-1} \text{ s}^{-1}$) that the major sink for these compounds in the atmosphere is thermal decomposition to the peroxyacyl radical followed by reaction with NO and subsequent decomposition to CO₂. By contrast, the OH reaction of MPAN is competitive with thermal decomposition (28). Here we confirm that MPAN is the key

intermediate in the isoprene and MACR systems in the formation of 2-MG and its corresponding low-volatility oligoesters in the aerosol phase. If a PAN-type compound is involved in the formation of aerosol-phase products, the aerosol yields should depend on the $[\text{NO}_2]/[\text{NO}]$ ratio, as this ratio determines whether the peroxyacyl radicals produced via thermal decomposition reform PANs or react with NO and decompose. With urban $[\text{NO}_2]/[\text{NO}]$ ratios typically around 7, SOA mass yields from isoprene and MACR previously measured at $[\text{NO}_2]/[\text{NO}]$ ratios around 1 could be underestimated (8). Experimentally, such high $[\text{NO}_2]/[\text{NO}]$ ratios are not achieved using HONO as an OH source, as NO is produced from both the synthesis of HONO and photolysis of HONO with UV irradiation.

6.4 Atmospheric Implications

The importance of IEPOX and MPAN in forming isoprene SOA under low- and high- NO_x conditions, respectively, provides significant insights into heretofore-unidentified aerosol precursors. In the presence of anthropogenic pollutants, such as NO_2 and acidic aerosol produced from the oxidation of SO_2 , SOA mass yields from isoprene under high- and low- NO_x conditions, respectively, increase substantially. As isoprene is estimated to be the largest single contributor to global SOA, these results may help to resolve two existing dilemmas in atmospheric chemistry: (1) radiocarbon (^{14}C) data consistently indicate that well over half of the ambient SOA is of modern (biogenic) origin (7, 33), whereas correlations between water-soluble organic carbon and anthropogenic tracers, such as CO, suggest that much of the SOA is actually of anthropogenic origin (34, 35); and (2) comparisons between measured and predicted SOA based on known precursors suggest that there is a substantial amount of “missing

urban SOA” not included in current models (35–37). Revising the chemistry of isoprene in regional and global SOA models could lead to a decrease in this discrepancy; however, the measurement and parameterization of aerosol acidity requires additional work.

6.5 Materials and Methods

6.5.1 Experimental details

The experiments were carried out in the Caltech dual 28-m³ FEP Teflon chambers (38). Seed aerosol is generated using a constant rate atomizer. Dilute solutions (concentrations of 0.06M or lower) of ammonium sulfate and magnesium sulfate with sulfuric acid are used for neutral and highly acidic seed aerosol, respectively. The particle number and volume concentrations are corrected for particle wall loss using size-dependent coefficients determined from loss of inert particles. Isoprene, MACR or MBO is added to the chamber by vaporizing a known volume of the hydrocarbon in a glass bulb. In the reactive uptake experiments (see Table 6.2 and Supporting Information), BEPOX is injected into the chamber by vaporizing a small (~30 mg) amount of the solid at ~60°C in a small glass vial and introducing the vapor into the chamber in a stream of N₂. The amount injected into the chamber is estimated by measuring the mass loss of BEPOX after injection. MPAN is injected in a similar manner in a -10°C ice-salt bath. At -10°C, dodecane has a negligible vapor pressure, and as a result, not expected to be introduced into the chambers. In low-NO_x photooxidation experiments (see Table 6.2 and Supporting Information), the photolysis of H₂O₂ is used to generate OH radicals. In order to prevent partitioning of H₂O₂ into the seed aerosol, all low-NO_x experiments were conducted under dry conditions (< 10% RH). At the relatively high mixing ratios of H₂O₂, significant HO₂ radical levels are produced by the OH + H₂O₂ reaction, which is

avored at the slow chamber photolysis rate of H_2O_2 . In high- NO_x photooxidation experiments, the photolysis of nitrous acid (HONO) is used as the OH precursor (see Table 6.3 and Supporting Information).

6.5.2 Gas-phase measurements

The concentrations of isoprene, MACR and MBO are monitored by a gas chromatograph equipped with a flame ionization detector (GC/FID, Agilent 6890N). NO/NO_x and O_3 are monitored by commercial chemiluminescence monitors (Horiba, APNA 360 and APOA 360, respectively). A custom-modified Varian 1200 CIMS was used to continuously monitor gas-phase species (3, Supporting Information).

6.5.3 Aerosol-phase measurements

Aerosol size distributions and volume concentrations are measured using a differential mobility analyzer (DMA, TSI 3081) with a condensation nuclei counter (CPC, TSI 3760). Aerosol samples are collected onto Teflon filters for off-line chemical characterization by both GC/EI-MS with prior trimethylsilylation and UPLC/ESI-TOFMS. Filter handling and extraction protocols in high-purity methanol have been described previously for aerosol samples analyzed by the UPLC/(-)ESI-TOFMS technique (18). Details of the sample preparation and operation protocols for the GC/EI-MS technique can be found in the Supporting Information. Selected SOA samples formed from the reactive uptake of BEPOX on either neutral or acidified sulfate seed aerosol were continuously sampled by a particle-into-liquid sampler (PILS) with subsequent offline analysis by ion chromatography (IC) (39).

6.5.4 Materials

Isoprene (Aldrich, 99%), MACR (Aldrich, 95%) and MBO (Aldrich, 98%) are obtained from commercial sources. BEPOX is synthesized following the procedure derived by Skinner et al. (40) (see Supporting Information). MPAN is synthesized from methacrylic anhydride (Aldrich, 94%) in dodecane (Sigma-Aldrich, 99+%, anhydrous) based on the method of Nouaime et al. (41) with a few modifications (see Supporting Information). The purity of the product is confirmed by gas-phase FTIR spectroscopy (see Supporting Information).

6.6 Acknowledgments

This work was supported by the Office of Science (Biological and Environmental Research), U.S. Department of Energy grant DE-FG02-05ER63983, and U.S. Environmental Protection Agency (EPA) STAR agreement RD-833749. The CIMS instrument was purchased as part of a major research instrumentation grant from the National Science Foundation (ATM-0619783); assembly and testing was supported by the Davidow Discovery Fund. We thank Andreas Kürten for assembling the CIMS instrument and John D. Crounse for synthesizing and characterizing (with H-NMR) the BEPOX. The Waters UPLC-LCT Premier XT time-of-flight mass spectrometer was purchased in 2006 with a grant from the National Science Foundation, Chemistry Research Instrumentation and Facilities Program (CHE-0541745). N.C.E. was supported by the Camille and Henry Dreyfus Postdoctoral Program in Environmental Chemistry. This work has not been formally reviewed by the EPA. The views expressed in this document are solely those of the authors, and the EPA does not endorse any products or commercial services mentioned in this publication. We also thank Magda Claeys for useful discussions.

6.7 Supporting Information

6.7.1 Experimental Details of Chamber Operation

6.7.1.1 Low-NO_x Experiments

280 μL of 50% H_2O_2 solution (Aldrich) is injected into a glass bulb, vaporized in a 30°C water bath, and introduced into the chamber in an air stream, resulting in an estimated chamber concentration of 4 ppmv. 50% of the available blacklights are used to irradiate the chambers.

6.7.1.2 High-NO_x Experiments

HONO is prepared by adding 1 wt% aqueous NaNO_2 dropwise into 10 wt% sulfuric acid, and introduced into the chamber using an air stream (42). NO or NO_2 are injected into the chambers from gas cylinders (Scott Marrin). 10% of the available blacklights are used to irradiate the chambers.

6.7.2 Procedures to Confirm Purity of MPAN

The purity of the MPAN sample was quantified by comparison of gas-phase FTIR spectra with those published in other studies (see MPAN synthesis below). The major impurity, methacrylic acid, does not contribute to SOA. We oxidized methacrylic acid under the same conditions used in the MPAN study and SOA formation was not observed. At the NO levels (>10 ppb) in the photooxidation experiments, $\text{RO}_2 + \text{HO}_2$ and $\text{RO}_2 + \text{RO}_2$ reactions do not compete with $\text{RO}_2 + \text{NO}$ or $\text{RO}_2 + \text{NO}_2$ reactions, and aerosol-phase formation of 2-MG from isoprene cannot be attributed to gas-phase RO_2 radical-cross reactions of methacrylic acid.

6.7.3 Details of the CIMS Technique

6.7.3.1 Operating Conditions

The CIMS was operated in negative ion mode where CF_3O^- is used as the reagent ion, and in positive ion mode of proton transfer mass spectrometry (PTR-MS) (43). In negative ion mode, CF_3O^- selectively clusters with compounds with high fluorine affinities to form a complex detected at $m/z = \text{MW}+85$, while highly acidic molecules will mainly form the transfer product detected at $m/z = \text{MW}+19$ (43). To distinguish between hydroxyisoprene hydroperoxide and isoprene epoxydiols (both of which are both detected at m/z 203), an MS/MS technique was used (3). In the first quadrupole the parent ion is selected, and in the second quadrupole a small amount of N_2 is present to act as a collision partner producing collision-induced daughter ions, which are subsequently selected in the third quadrupole. Depending on the nature of the ion, different collision-induced daughter ions can be formed. Two daughter ions of particular interest are at m/z 63 and m/z 183. The daughter ion at m/z 63 is selective for the hydroperoxide group, while the isoprene epoxydiols fragment in sufficient yield at m/z 183. In PTR-MS mode, residual H_2O in N_2 is reacted with N_2^+ ions to form $\text{H}^+\cdot(\text{H}_2\text{O})_n$ reagent ions.

6.7.3.2 Correction of the MS/MS daughter ion signal associated to IEPOX

ISPOOH and IEPOX are isomers, and as a result, are both detected at m/z 203. As noted above, using the MS/MS technique of the CIMS, these isomers can be separated from each other due to their production of different characteristic daughter ions. It has also been shown that IEPOX does not interfere with the daughter ion at m/z 63 associated to ISPOOH. IEPOX is known to fragment in good yield to m/z 183; however, ISPOOH also fragments to this ion to a lesser extent. In order to determine the extent that ISPOOH fragments to m/z 183 in the second quadrupole, a large number of the daughter ions from the parent ion at m/z 203 were analyzed and it was determined that

only two compounds were present at this ion (i.e., ISPOOH and IEPOX). Next, the data from an experimental run where ISPOOH was only present in the gas phase was analyzed to determine the amount of the daughter ion at m/z 183 that was from ISPOOH. It was found that 20% of the daughter ion at m/z 183 was from ISPOOH and this amount was subtracted from all MS/MS spectra of m/z 183 so that only IEPOX was displayed. This corrected signal was also used to determine the concentration of IEPOX.

6.7.4 Filter Extraction and Operation Protocols for the GC/EI-MS Technique

Filter extractions for aerosol samples analyzed by the GC/EI-MS technique are similar to the UPLC/(-)ESI-TOFMS technique; however, following the removal of the methanol extraction solvent with ultra-high purity N_2 , the dried residue was trimethylsilylated by the addition of 100 mL of BSTFA + trimethylchlorosilane (99:1 (v/v), Supleco) and 50 mL of pyridine (Sigma-Aldrich, 98%, anhydrous), and the resultant mixture was heated for an hour at 70 °C. This latter step converted all isoprene SOA constituents containing carboxyl and hydroxyl functions into volatile trimethylsilyl (TMS) derivatives. GC/EI-MS analyses of the TMS derivatives were performed with a system comprised of a Hewlett Packard (HP) 5890 Series 2 Plus chromatograph, interfaced to a HP 5972 Series mass selective detector. A Restek RTX-5MS fused-silica capillary column (5% diphenyl, 95% dimethyl polysiloxane, 0.25 mm film thickness, 30 m x 0.25 mm i.d.) was used to separate the TMS derivatives before MS detection. 1 mL aliquots of each sample were injected in the splitless mode onto the column by a HP 7673 Series GC injector and autosampler. Helium was used as the carrier gas at a flow rate of 0.8 mL min⁻¹. The 65.17 min temperature program of the GC was as follows: isothermal hold at 60 °C for 1 min, temperature ramp of 3 °C min⁻¹ up to 200 °C, isothermal hold at

200 °C for 2 min, temperature ramp of 20 °C min⁻¹ to 310 °C, and isothermal hold at 310 °C for 10 min. The MS scan was performed in the m/z 50–500 range. A solvent delay time of 7.5 min was employed. The ion source was operated at an electron energy of 70 eV. The temperatures of both the GC inlet and detector were at 250 °C.

6.7.5 Materials

6.7.5.1 BEPOX synthesis

In general, an aqueous solution of 2-butene-1,4-diol (Fluka, purum, ≥98.0%) is reacted with H₂O₂ catalyzed by tungstic acid, followed by removal of H₂O and other impurities. NMR of the final product reveals purity greater than 95% and the product is used as is.

6.7.5.2 MPAN synthesis

Methanesulfonic acid (Fluka, puriss., ≥99.0%) is used in place of sulfuric acid as suggested by Williams et al. (44) to improve the purity of the product. No column purification is carried out. Instead, the MPAN solution is purified by 20–25 successive washes with deionized water (Millipore, 18.2 MΩ•cm). Spectra of the MPAN sample showed strong peaks at 1065, 1297, 1740, 1807 cm⁻¹, which are associated with MPAN (29). No peaks associated with methacrylic anhydride and methacrylic acid are observed in spectra obtained from the MPAN sample.

6.8 References

1. Guenther A, et al. (2006) Estimates of global terrestrial isoprene emissions using MEGAN (Model of Emissions of Gases and Aerosols from Nature). *Atmos Chem Phys* 6:3181–3210.
2. Lelieveld J, et al. (2008) Atmospheric oxidation capacity sustained by a tropical forest. *Nature* 452:737–740.

3. Paulot F, et al. (2009) Unexpected epoxide formation in the gas-phase photooxidation of isoprene. *Science* 325:730–733.
4. Chameides W, Lindsay R, Richardson J, Kiang C (1988) The role of biogenic hydrocarbons in urban photochemical smog: Atlanta as a case study. *Science* 241:1473–1475.
5. Claeys M, et al. (2004) Formation of secondary organic aerosols through photooxidation of isoprene. *Science* 303:1173–1176.
6. Henze DK, et al. (2008) Global modeling of secondary organic aerosol formation from aromatic hydrocarbons: high- vs. low-yield pathways. *Atmos Chem Phys* 8:2405–2421.
7. Hallquist M, et al. (2009) The formation, properties and impact of secondary organic aerosol: current and emerging issues. *Atmos Chem Phys* 9:5155–5236.
8. Carlton AG, Wiedinmyer C, Kroll JH (2009) A review of Secondary Organic Aerosol (SOA) formation from isoprene. *Atmos Chem Phys* 9:4987–5005.
9. Kroll JH, Ng NL, Murphy SM, Flagan RC, Seinfeld JH (2006) Secondary organic aerosol formation from isoprene photooxidation. *Environ Sci Technol* 40:1869–1877.
10. Presto AA, Hartz KEH, Donahue NM (2005) Secondary organic aerosol production from terpene ozonolysis 2. Effect of NO_x concentration. *Environ Sci Technol* 39:7046–7054.
11. Kroll JH, Seinfeld JH (2008) Chemistry of secondary organic aerosol: Formation and evolution of low-volatility organics in the atmosphere. *Atmos Environ* 42:3593–3624.
12. Surratt JD, et al. (2006) Chemical composition of secondary organic aerosol formed from the photooxidation of isoprene. *J Phys Chem A* 110:9665–9690.
13. Lim YB, Ziemann PJ (2009) Chemistry of secondary organic aerosol formation from OH radical-initiated reactions of linear, branched, and cyclic alkanes in the presence of NO_x. *Aerosol Sci Technol* 43:604–619.
14. Edney EO, et al. (2005) Formation of 2-methyl tetrols and 2-methylglyceric acid in secondary organic aerosol from laboratory irradiated isoprene/NO_x/SO₂/air mixtures and their detection in ambient PM_{2.5} samples collected in the eastern United States. *Atmos Environ* 39:5281–5289.
15. Surratt JD, et al. (2007) Effect of acidity on secondary organic aerosol formation from isoprene. *Environ Sci Technol* 41:5363–5369.

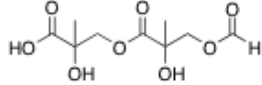
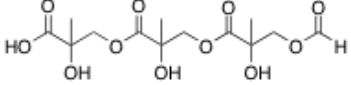
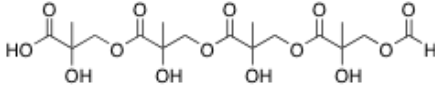
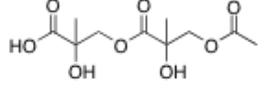
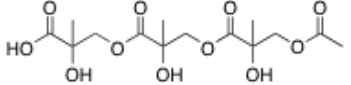
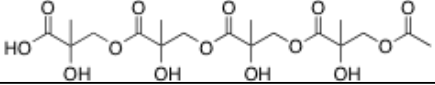
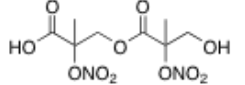
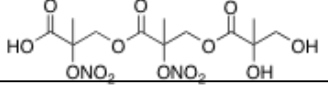
16. Surratt JD, et al. (2007) Evidence for organosulfates in secondary organic aerosol. *Environ Sci Technol* 41:517–527.
17. Gómez-González Y, et al. (2008) Characterization of organosulfates from the photooxidation of isoprene and unsaturated fatty acids in ambient aerosol using liquid chromatography/(-)electrospray ionization mass spectrometry. *J Mass Spectrom* 43:371–383.
18. Surratt JD, et al. (2008) Organosulfate formation in biogenic secondary organic aerosol. *J Phys Chem A* 112:8345–8378.
19. Minerath EC, Elrod MJ (2009) Assessing the potential for diol and hydroxy sulfate ester formation from the reaction of epoxides in tropospheric aerosols. *Environ Sci Technol* 43:1386–1392.
20. Wang W, et al. (2005) Characterization of oxygenated derivatives of isoprene related to 2-methyltetrols in Amazonian aerosols using trimethylsilylation and gas chromatography/ion trap mass spectrometry. *Rapid Commun Mass Spectrom* 19:1343–1351.
21. Kleindienst TE, Lewandowski M, Offenberg JH, Jaoui M, Edney EO (2009) The formation of secondary organic aerosol from the isoprene + OH reaction in the absence of NO_x. *Atmos Chem Phys* 9:6541–6558.
22. Ren X, et al. (2003) Intercomparison of peroxy radical measurements at a rural site using laser-induced fluorescence and Peroxy Radical Chemical Ionization Mass Spectrometer (PerCIMS) techniques. *J Geophys Res* 108(D19):4605.
23. Atkinson R, et al. (2006) Evaluated kinetic and photochemical data for atmospheric chemistry: Volume II – gas phase reactions of organic species. *Atmos Chem Phys* 6:3625–4055.
24. Iinuma Y, Böge O, Kahnt A, Herrmann H (2009) Laboratory chamber studies on the formation of organosulfates from reactive uptake of monoterpene oxides. *Phys Chem Chem Phys* 11:7985–7997.
25. Tuazon EC, Atkinson R (1990) Product study of the gas-phase reaction of isoprene with OH radical in the presence of NO_x. *Int J Chem Kinet* 22:1221–1236.
26. Szmigielski R, et al. (2007) Characterization of 2-methylglyceric acid oligomers in secondary organic aerosol formed from the photooxidation of isoprene using trimethylsilylation and gas chromatography/ion trap mass spectrometry. *J Mass Spectrom* 42:101–116.
27. Tuazon EC, Atkinson R (1990) A product study of the gas-phase reaction of methacrolein with the OH radical in the presence of NO_x. *Int J Chem Kinet* 22:591–602.

28. Orlando JJ, Tyndall GS, Paulson SE (1999) Mechanism of the OH-initiated oxidation of methacrolein. *Geophys Res Lett* 26:2191–2194.
29. Bertman SB, Roberts JM (1991) A PAN analog from isoprene photooxidation. *Geophys Res Lett* 18:1461–1464.
30. Paulot F, et al. (2009) Isoprene photooxidation: new insights into the production of acids and organic nitrates. *Atmos Chem Phys* 9:1479–1501.
31. Roberts JM, Bertman SB (1992) The thermal decomposition of peroxyacetic nitric anhydride (PAN) and peroxyethacrylic nitric anhydride (MPAN). *Int J Chem Kinet* 24:297–307.
32. Dommen J, et al. (2006) Laboratory observation of oligomers in the aerosol from isoprene/NO_x photooxidation. *Geophys Res Lett* 33:L13805.
33. Schichtel BA, et al. (2008) Fossil and contemporary fine particulate carbon fractions at 12 rural and urban sites in the United States. *J Geophys Res* 113:D02311.
34. Weber RJ, et al. (2007) A study of secondary organic aerosol formation in the anthropogenic-influenced southeastern United States. *J Geophys Res* 112:D13302.
35. de Gouw JA, et al. (2005) Budget of organic carbon in a polluted atmosphere: Results from the New England Air Quality Study in 2002. *J Geophys Res* 110:D16305.
36. Heald CL, et al. (2005) A large organic aerosol source in the free troposphere missing from current models. *Geophys Res Lett* 32:L18809.
37. Volkamer R, et al. (2006) Secondary organic aerosol formation from anthropogenic air pollution: Rapid and higher than expected. *Geophys Res Lett* 33:L17811.
38. Keywood MD, Varutbangkul V, Bahreini R, Flagan RC, Seinfeld JH (2004) Secondary organic aerosol formation from the ozonolysis of cycloalkenes and related compounds. *Environ Sci Technol* 38:4157–4164.
39. Sorooshian A, et al. (2006) Modeling and characterization of a particle-into-liquid sampler (PILS). *Aerosol Sci Technol* 40:396–409.
40. Skinner JR, Wilcoxon CH, Carlson GJ (1958) Production of epoxides. *United States Patent Office* 2,833,788.
41. Nouaime G, et al. (1998) Sequential oxidation products from tropospheric isoprene chemistry: MACR and MPAN at a NO_x-rich forest environment in the southeastern United States. *J Geophys Res* 103(D17):22463–22471.

42. Chan AWH, et al. (2009) Secondary organic aerosol formation from photooxidation of naphthalene and alkyl naphthalenes: implications for oxidation of intermediate volatility organic compounds (IVOCs). *Atmos Chem Phys* 9:3049–3060.
43. Crounse JD, McKinney KA, Kwan AJ, Wennberg PO (2006) Measurements of gas-phase hydroperoxides by chemical ionization mass spectrometry. *Anal Chem* 78:6726–6732.
44. Williams J, et al. (2000) A method for the airborne measurement of PAN, PPN, and MPAN. *J Geophys Res* 105(D23):28943–28960.

Table 6.1. High-NO_x MPAN SOA Constituents

	[M – H] [–] ion	UPLC/ESI- TOFMS Measured Mass	TOFMS Suggested Ion Formula	Error (mDa)	i-Fit	Structure ^a
Oligoester Series 1	221	221.0661	C ₈ H ₁₃ O ₇ [–]	1.6	0.3	
	323	323.0979	C ₁₂ H ₁₉ O ₁₀ [–]	0.1	22.6	
	425	425.1290	C ₁₆ H ₂₅ O ₁₃ [–]	-0.5	48.0	
Oligoester Series 2	266	266.0507	C ₈ H ₁₂ NO ₉ [–]	-0.5	32.8	
	368	368.0831	C ₁₂ H ₁₈ NO ₁₂ [–]	0.2	11.4	
	470	470.1149	C ₁₆ H ₂₄ NO ₁₅ [–]	0.3	56.3	
	572	572.1510	C ₂₀ H ₃₀ NO ₁₈ [–]	4.7	1.0	

Oligoester Series 3 ^b	249	249.0616	C ₉ H ₁₃ O ₈ ⁻	0.6	2.7	
	351	351.0912	C ₁₃ H ₁₉ O ₁₁ ⁻	-1.5	46.9	
	453	453.1248	C ₁₇ H ₂₅ O ₁₄ ⁻	0.4	63.7	
Oligoester Series 4 ^c	263	263.0740	C ₁₀ H ₁₅ O ₈ ⁻	-2.7	4.7	
	365	365.1061	C ₁₄ H ₂₁ O ₁₁ ⁻	-2.3	54.9	
	467	467.1434	C ₁₈ H ₂₇ O ₁₄ ⁻	3.3	23.7	
Oligoester Series 5	311	311.0333	C ₈ H ₁₁ N ₂ O ₁₁ ⁻	-3.0	58.9	
	413	413.0664	C ₁₂ H ₁₇ N ₂ O ₁₄ ⁻	-1.6	71.9	

^a For simplicity, only one isomer is shown.

^b This oligoester series involves the esterification with formic acid.

^c This oligoester series involves the esterification with acetic acid.

Table 6.2. Summary of experimental conditions for low-NO_x experiments.

HC ^{a,b}	[HC] ₀ (ppb)	OH precursor	Seed Aerosol ^c	Seed volume (μm ³ cm ⁻³)	RH (%)	SOA volume (μm ³ cm ⁻³) ^d	SOA mass (μg m ⁻³) ^e	injection order
BEPOX	9	none	neutral	^f	4	^f	^f	BEPOX then seed
isoprene	40	H ₂ O ₂	highly acidic	14.5	6	21.3	31.8	all reactants present at start
isoprene	49	H ₂ O ₂	neutral	16.5	12	1.1	1.7	all reactants present at start
BEPOX	7	none	highly acidic	^f	5	^f	^f	BEPOX then seed
3-butene-1,2-diol	100 ^g	none	highly acidic	^f	12	^f	^f	butenediol then seed
BEPOX	^f	none	neutral	9.7	7	0.4	0.9	seed then BEPOX
BEPOX	^f	none	highly acidic	17.9	9	10.2	15.8	seed then BEPOX
butadiene	100 ^g	H ₂ O ₂	highly acidic	^f	11	^f	^f	2.5 hours oxidation then seed

^a HC = hydrocarbon; BEPOX = 2,3-epoxy-1,4-butanediol^b Temperatures = 294-299 K.^c neutral = (NH₄)₂SO₄; highly acidic = MgSO₄ + H₂SO₄^d not corrected for wall loss^e corrected for wall loss, assuming density of 1.4^f not available owing to order of injection^g estimated based on amount injected

Table 6.3. Summary of experimental conditions for the high-NO_x experiments.

HC ^{a,b}	[HC] ₀ (ppb)	OH precursor	additional NO _x	[NO] ₀ (ppb)	[NO ₂] ₀ (ppb)	[NO ₂] ₀ /[NO] ₀	RH (%)	seed (μm ³ cm ⁻³)	SOA volume (μm ³ cm ⁻³) ^c	SOA mass (μg m ⁻³) ^d
methacrolein	277	HONO	+NO	725	365	0.5	9	11.4	5.2	10.1
methacrolein	285	HONO	+NO ₂	296	692	2.3	9	12.3	12.8	24.5
methacrolein	257	HONO	+NO	527	407	0.8	9	12.1	8.5	14.4
MPAN ^e		HONO	none	177	260	1.5	9	7.6	66.4	118
MBO	218	H ₂ O ₂	+NO+NO ₂	198	177	0.9	10	11.1	<2	<2
methacrylic acid	100	HONO	none	313	461	1.5	9	12.3	<2	<2
isoprene	523	HONO	none	312	510	1.6	9	10.8	41.7	65.2

^a HC = hydrocarbon; MPAN = methacryloylperoxynitrate; MBO = 2-methyl-3-buten-2-ol

^b Temperatures = 295-296 K

^c not corrected for wall loss

^d corrected for wall loss, assuming density of 1.4

^e not measured

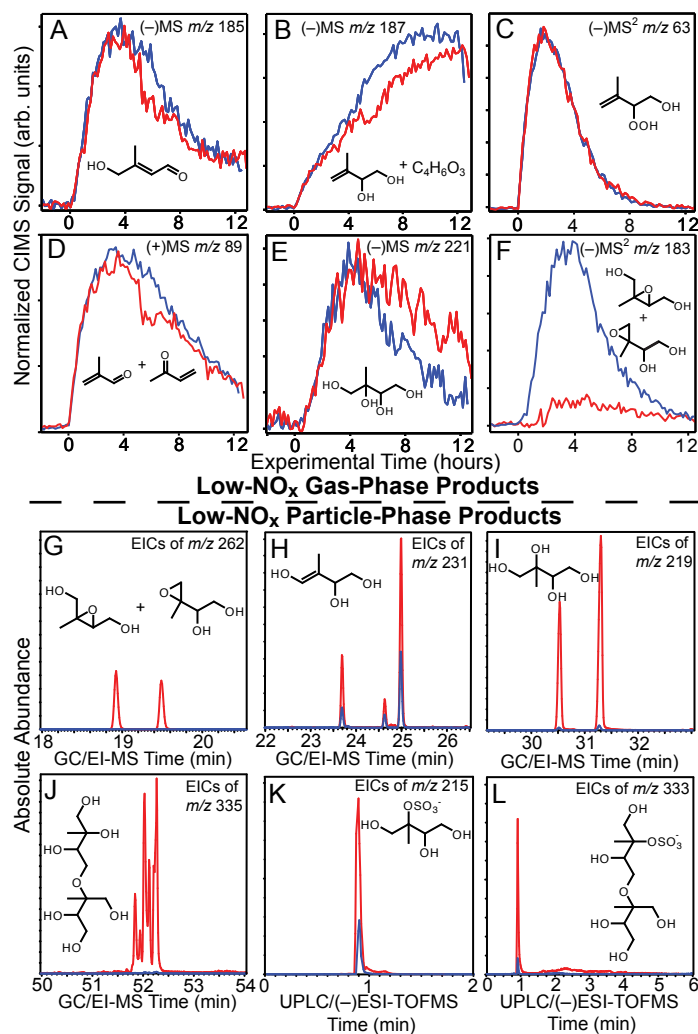


Figure 6.1. Comparison of important gas- and particle-phase products produced from isoprene under low-NO_x conditions in the presence of either neutral (blue lines) or highly acidified (red lines) sulfate seed aerosol. In most cases, only one structural isomer is shown.

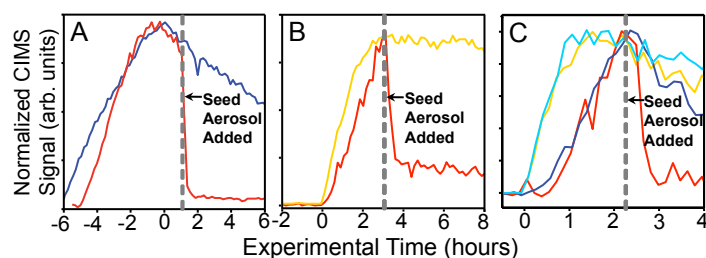


Figure 6.2. (-)CIMS time traces: (A) Reactive uptake of gas-phase BEPOX in the presence of either neutral (blue line) or highly acidified (red line) sulfate seed aerosol under dark conditions. (B) Hydroxy hydroperoxide (orange line) and BEPOX (red line) produced from butadiene under low- NO_x conditions. (C) ISOPOOH (neutral seed = light blue line; highly acidic seed = orange line) and IEPOX (neutral seed = blue line; highly acidic seed = red line) produced from isoprene under low- NO_x conditions. Signals of the IEPOX are normalized to that of the ISOPOOH when lights are turned off.

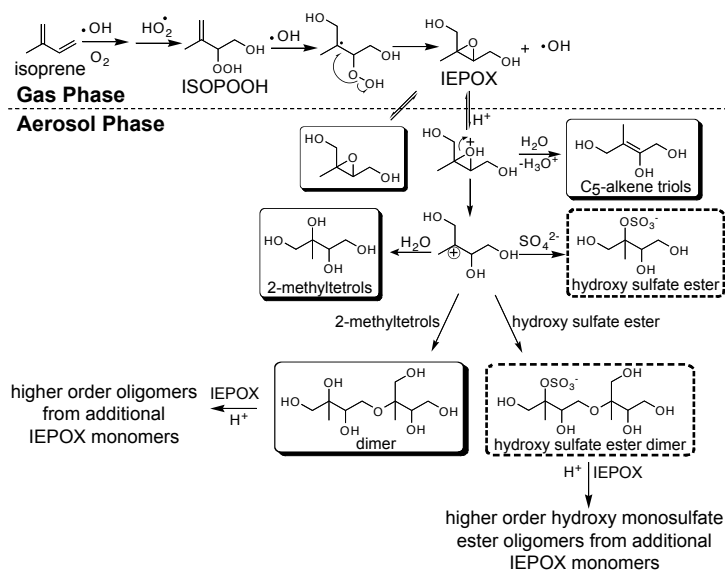


Figure 6.3. Mechanism for the enhancement of SOA formation from isoprene under lower- NO_x conditions due to increased aerosol acidity. SOA constituents in shaded and dashed boxes are observed by GC/MS and UPLC/(-)ESI-TOFMS, respectively. Only the β -IEPOX is considered here, but this also applies to δ -IEPOX.

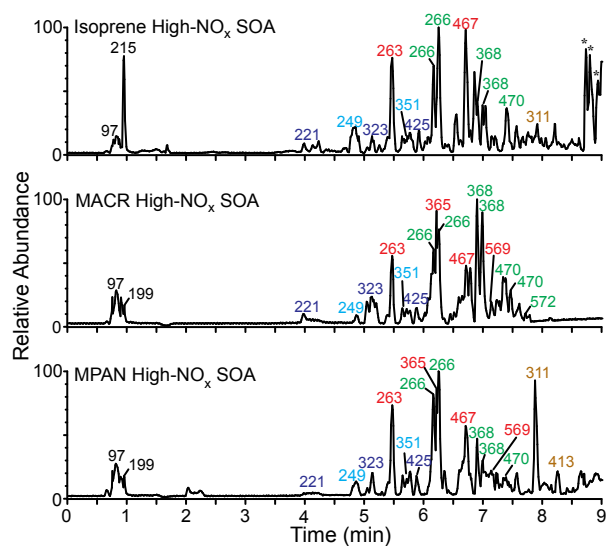


Figure 6.4. UPLC/(-)ESI-TOFMS BPCs. The numbers listed above each peak correspond to the respective $[M - H]^-$ base peak ions. Similar colored $[M - H]^-$ ions are of the same oligoester series (Table 6.1). m/z 97, 199, and 215 correspond to sulfate, an organosulfate of 2-MG (16), and an organosulfate of 2-methyltetrols (15, 16), respectively.

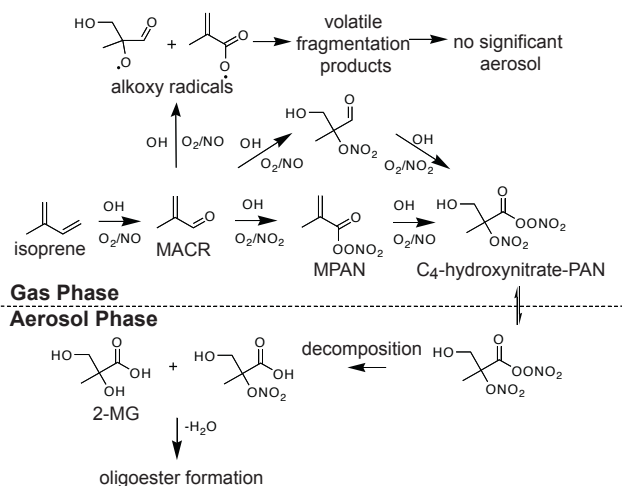


Figure 6.5. Possible chemical mechanism for the formation of isoprene SOA under high- NO_x conditions. Detailed chemical structures of the high- NO_x SOA constituents resulting from the oligoester formation can be found in Table 6.1.

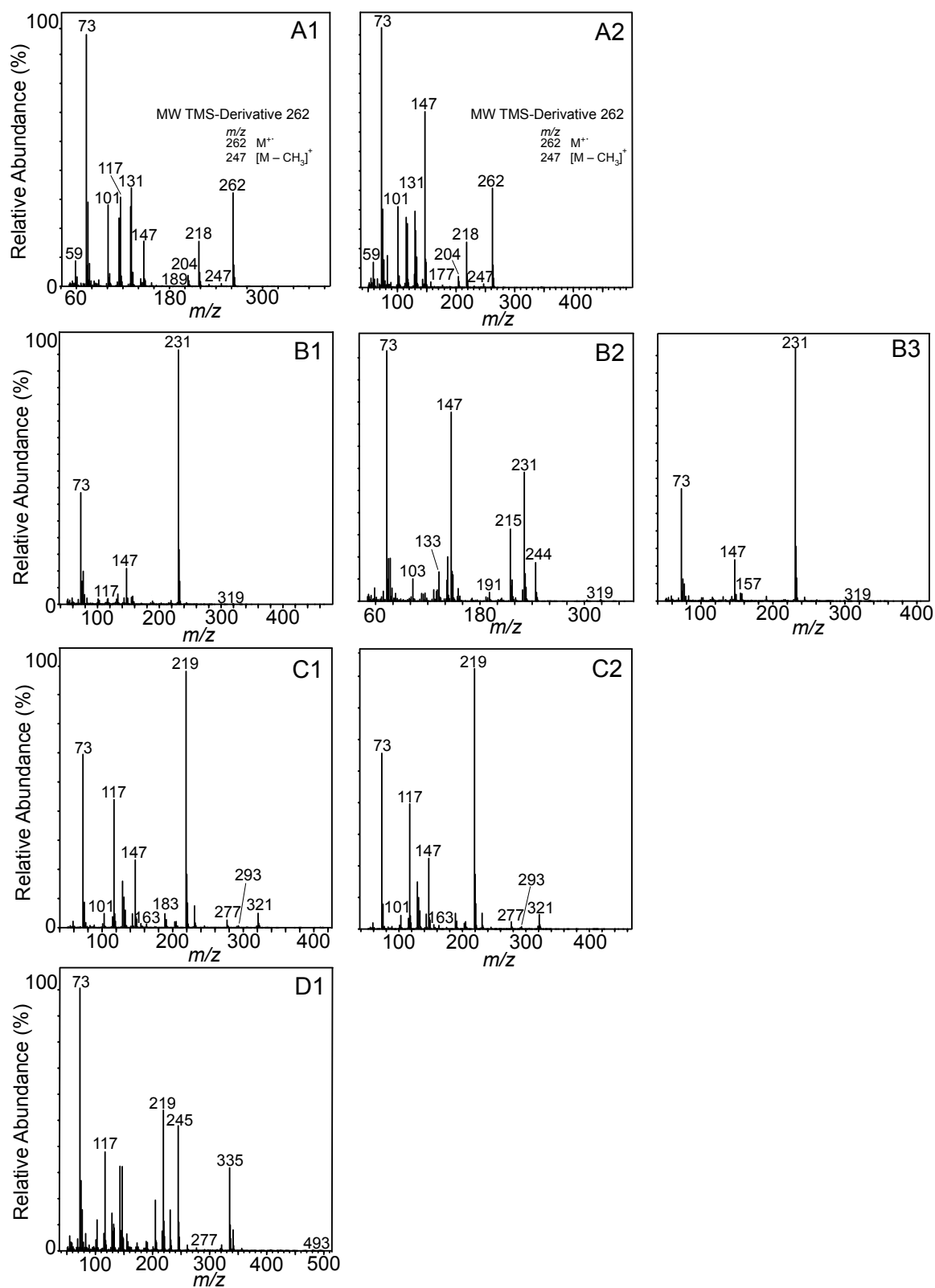


Figure 6.6. GC/EI-MS mass spectra for isoprene low- NO_x SOA constituents formed in the highly acidified sulfate seed aerosol experiment chemically characterized in Figure

6.1*G–J*. (A1–A2) Mass spectra corresponding to the IEPOX compounds characterized for the first time in low-NO_x isoprene SOA. (B1–B3) Mass spectra corresponding to the three isomers of the C₅-alkene triols. (C1–C2) Mass spectra corresponding to the diastereoisomeric 2-methyltetrols. (D1) Averaged mass spectrum corresponding to all 6 major isomers of the previously characterized hemiacetal dimers.

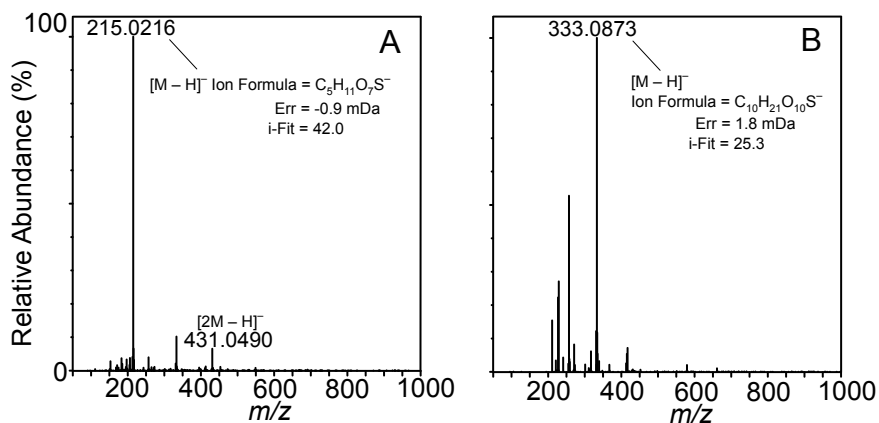


Figure 6.7. UPLC/(-)ESI-TOFMS mass spectra for isoprene low- NO_x SOA constituents formed in the highly acidified sulfate seed aerosol experiment chemically characterized in Figure 6.1K and Figure 6.1L, respectively. (A) Mass spectrum corresponding to the organosulfate derivative of the 2-methyltetrols (B) Mass spectrum corresponding to the organosulfate derivative of the dimer (denoted in prior work as the organosulfate of the hemiacetal dimer). These mass spectra are consistent with prior work (16, 17).

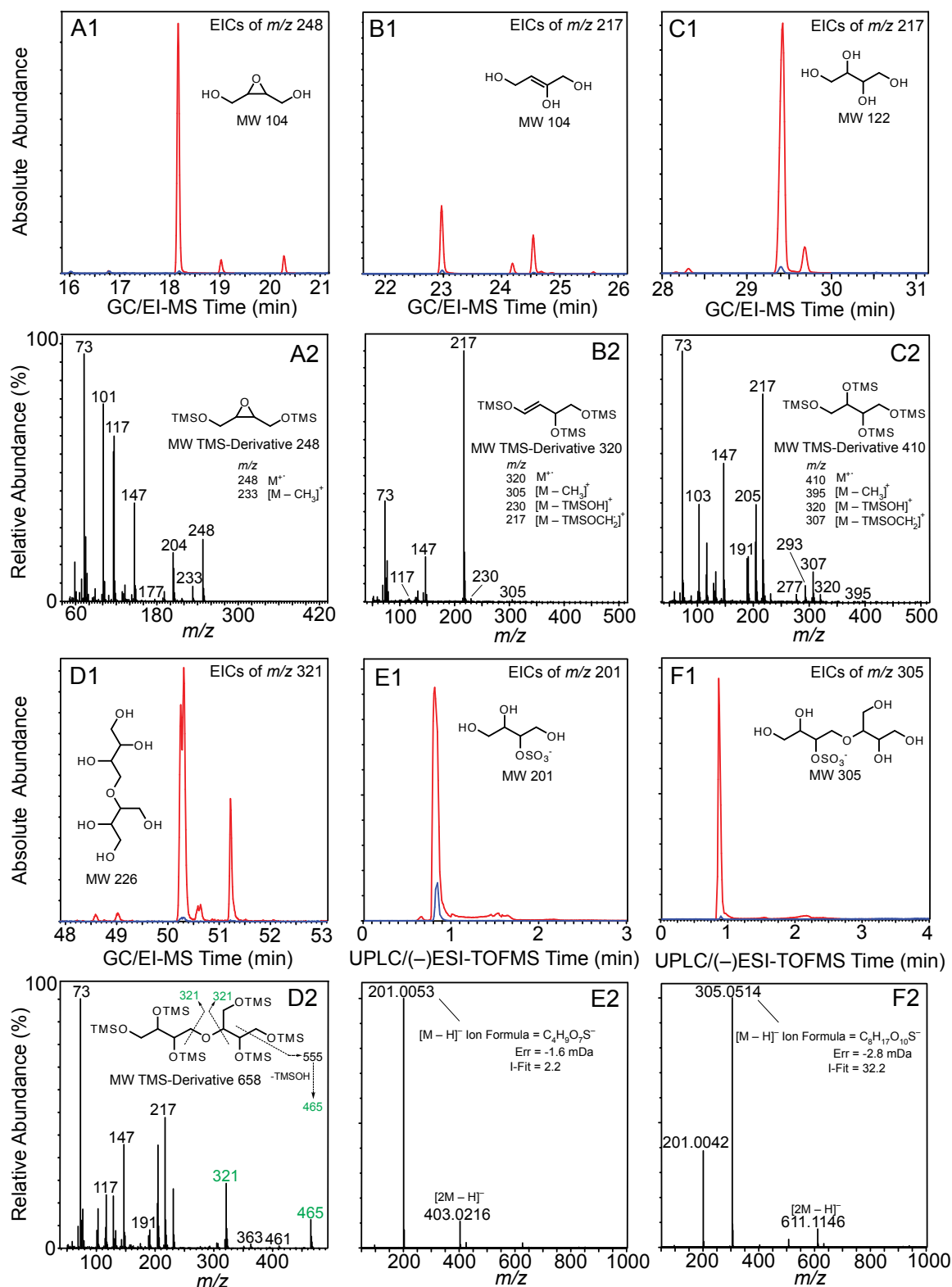


Figure 6.8. (A1–F1) Particle-phase constituents formed from the dark reactive uptake of BEPOX in the presence of either neutral (blue lines) or highly acidic (red lines) sulfate seed aerosol. (A2–F2) Corresponding mass spectra for each chemically characterized

particle-phase constituent shown in A1–F1. For simplicity, the mass spectra shown are only those of the most abundant isomers (chromatographic peaks) found in the EICs of A1–F1. All particle-phase constituents shown in A1–F1 are more abundantly formed from the uptake of the BEPOX in the presence of highly acidic sulfate seed aerosol, which is consistent with the low-NO_x isoprene SOA constituents shown in Figure 6.1. The particle-phase products characterized here were also observed in photooxidation of butadiene under low-NO_x conditions and in the presence of highly acidified sulfate seed aerosol. These data further confirm the role of IEPOX in forming low-NO_x isoprene SOA under acidic conditions.

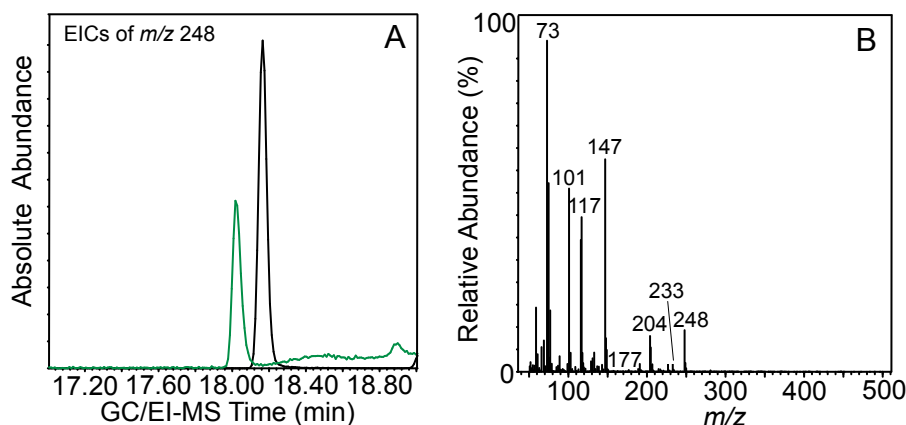


Figure 6.9. (A) GC/MS EICs of m/z 248 from 50 mg of BEPOX dissolved in 0.5 mL of 0.1 M H_2SO_4 in water (green line) and a reactive uptake experiment of BEPOX in the presence of highly acidified sulfate seed aerosol (black line). The two chromatographic peaks differ only slightly in terms of retention time owing to the samples being analyzed by the GC/EI-MS technique on separate days. (B) Corresponding mass spectrum for the chromatographic peak shown in A for the 50 mg BEPOX standard dissolved in 0.5 mL of 0.1 M H_2SO_4 in water (green line). The mass spectrum corresponding to the chromatographic peak shown in A for the reactive uptake experiment of BEPOX in the presence of highly acidified sulfate seed aerosol (black line) is presented in Figure 6.8A2. This comparison shows that some of the BEPOX remains unreacted in the particle phase and could have resulted there due to semi-volatile partitioning.

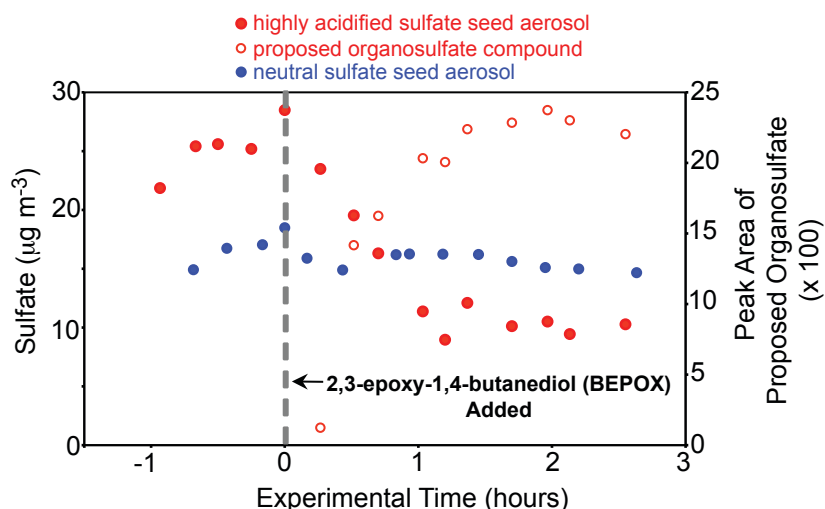


Figure 6.10. PILS/IC time traces of sulfate aerosol mass concentrations observed in experiments examining the reactive uptake of BEPOX in the presence of either neutral or highly acidified sulfate seed aerosol. In addition, a PILS/IC time trace is shown for the peak area of a tentatively assigned organosulfate compound observed only in the SOA formed from the reactive uptake of BEPOX in the presence of highly acidified sulfate seed aerosol. In both the neutral and highly acidified sulfate aerosol experiments, the seed aerosol was injected first and allowed to stabilize. Time zero indicates when the BEPOX was injected. The sulfate aerosol mass concentration decayed by ~58% of its initial loading 1 h after the BEPOX was injected in the presence of highly acidified sulfate seed aerosol. The sulfate aerosol mass concentration remained relatively constant after the injection of BEPOX in the presence of neutral sulfate seed aerosol. The large decay of sulfate mass in the highly acidified sulfate seed aerosol experiment indicates that it is lost due to reaction with BEPOX.

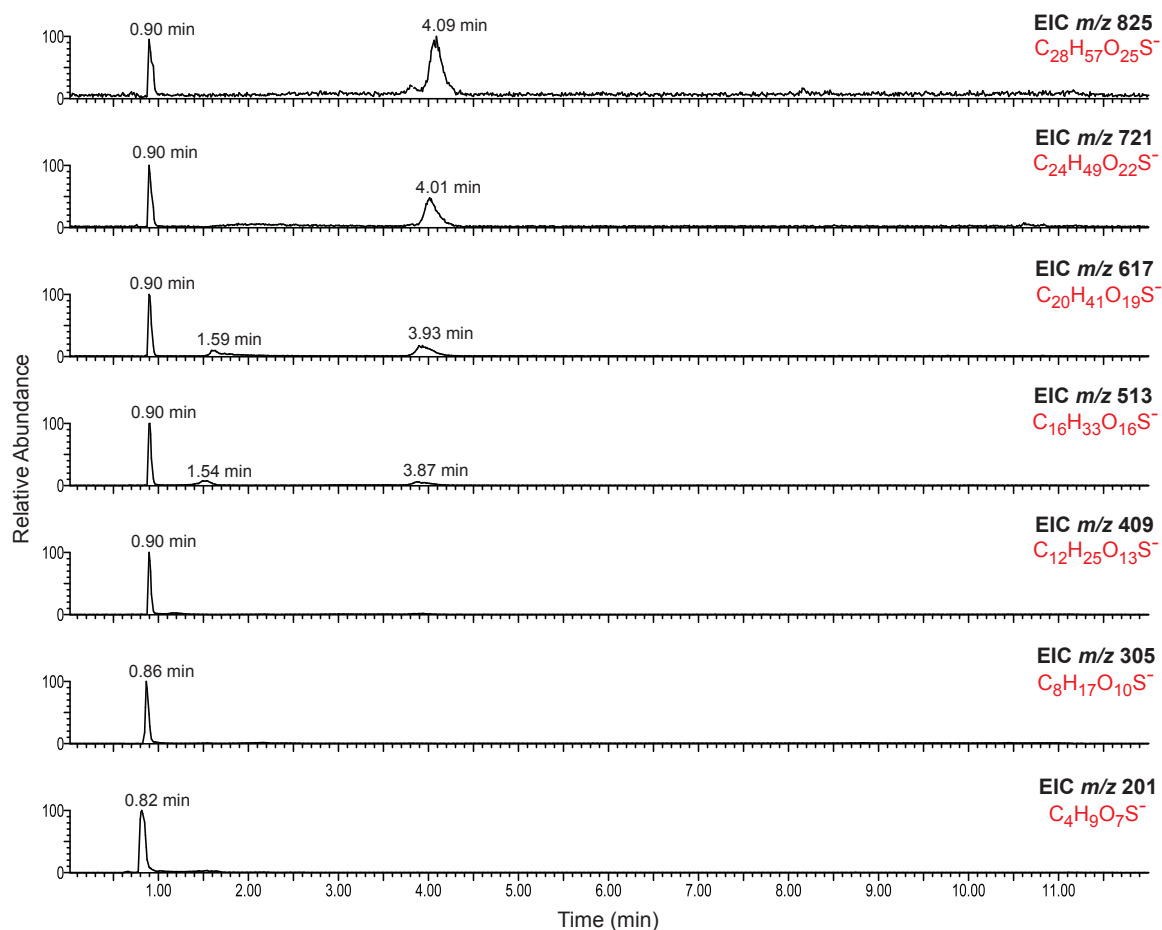


Figure 6.11. UPLC/(-)ESI-TOFMS EICs of organosulfates formed from the reactive uptake of BEPOX in the presence of highly acidified sulfate seed aerosol. EICs of m/z 409 to 825 indicate the formation of high-order (MW) organosulfates. Accurate mass measurements for each observed ion allowed for the determination and verification for the presence of the latter compounds by providing elemental composition (i.e., molecular formula) information. The elemental compositions for each ion are denoted in red. Numbers marked above the chromatographic peaks are the retention times for these compounds.

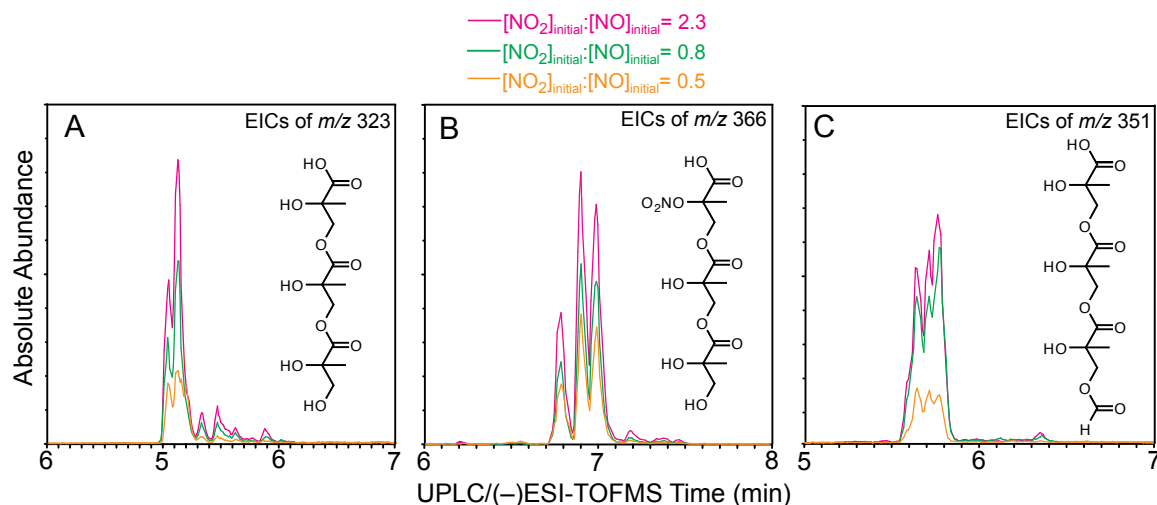


Figure 6.12. UPLC/(-)ESI-TOFMS EICs associated with three major classes of oligoesters previously observed in isoprene high- NO_x SOA (12, 26). For simplicity, only one structural isomer is shown in each of these EICs. These EICs were obtained from three different experiments in which the photooxidation of the same mixing ratio of MACR was conducted with varying levels of initial $[\text{NO}_2]/[\text{NO}]$ ratio. Increasing the initial $[\text{NO}_2]/[\text{NO}]$ ratio for these high- NO_x MACR experiments shown here results in the enhancement of both the previously characterized high- NO_x SOA constituents and the high- NO_x SOA masses. These enhancements are due to the formation and further reaction of MPAN under high- NO_2 conditions.